https://doi.org/10.5194/acp-2021-40
Preprint. Discussion started: 1 June 2021


Atmospheric Chemistry and Physics Discussions

# Observations of Aerosol-Vapor Pressure Deficit-Evaporative Fraction coupling over India

Chandan Sarangi[1,2]*, Tirthankar Chakraborty [3,4], Sachchidanand Tripathi [1,3]*, Mithun Krishnan[1], Ross Morrison[5], Jonathan Evans[5], Lina Mercado [5,6]

Affiliations:
[1] Department of Civil engineering, Indian Institute of Technology, Kanpur, Kanpur, India
[2] Department of Civil engineering, Indian Institute of Technology, Madras, Chennai, India
[3] Center for Environmental Science and Engineering, Indian Institute of Technology, Kanpur
[4] School of the Environment, Yale University
[5] UK Centre for Ecology & Hydrology, Wallingford, UK
[6] Department of Geography, University of Exeter, UK

* Corresponding authors: snt@iitk.ac.in and chandansarangi@iitm.ac.in

## Abstract

North India is a densely populated subtropical region with heavy aerosol loading, frequent heatwaves and strong atmosphere-biosphere coupling, making it ideal for studying the impacts of aerosols and temperature variation on latent heat flux (LH) and evaporative fraction (EF). Here, using in situ observations during the onset of the summer monsoon over a semi-natural grassland site in this region, we confirm that strong co-variability exists among aerosols, LH, air temperature ($T_{air}$) and vapor pressure deficit (VPD). Since the surface evapotranspiration is strongly controlled by both physical (available energy and moisture demand) and physiological (canopy and aerodynamic resistance) factors, we separately analyze our data for different combinations of aerosols and $T_{air}$/VPD changes. We find that aerosol loading and heatwave conditions both reduces SH. Further, we find that an increase in atmospheric VPD, tends to decrease the gross primary production (GPP) and thus LH, most likely as a response to stomatal closure of the dominant grasses at this location. In contrast, under heavy aerosol loading, LH is enhanced partly due to the physiological control exerted by the diffuse radiation fertilization effect (thus increasing EF). Moreover, LH and EF are positively associated with aerosol loading even under heatwave conditions, indicating a decoupling of plant's response to VPD enhancement (stomatal closure) in presence of high aerosol conditions. With heat-stress, VPD and aerosols expected to increase in future India, our results warrant in-depth analysis of aerosol-plant-temperature-EF continuum and its impact on Indian monsoon dynamics and crop vulnerability.

**Highlights:**

1. A rigorous analysis of Aerosol-EF-VPD coupling using collocated direct observations is presented
2. Increased aerosol loading enhances Evaporative Fraction by decreasing sensible heat and increasing latent heat.
3. Aerosols modulate the response of vegetation to changes in VPD under heatwave conditions

https://doi.org/10.5194/acp-2021-40
Preprint. Discussion started: 1 June 2021


Atmospheric Chemistry and Physics Discussions

**Keywords:** Grassland, Aerosol loading, eddy covariance, evaporative fraction, physiological response, diffuse radiation, Indo Gangetic Plains, heatwave, sensible heat, latent heat, Bowen ratio

## Introduction:

The surface energy balance represents the balance between the net incoming shortwave and longwave radiation (NR) flux at the Earth's surface and the partitioning of NR into latent heat (LH), sensible heat (SH) and ground heat (GH) fluxes [Wang and Dickinson, 2012]**.** While the dominant partitioning of energy as SH enhances the near-surface air temperature, the LH flux cools the surface and increases the moisture content of the boundary layer. Thus, perturbations to the partitioning of the outgoing turbulent energy fluxes from the land surface modify the near surface micrometeorology. One way of representing this partitioning is the evaporative fraction (EF=LH/(SH+LH)), or the proportion of the total available energy (NR-GH) available at the surface released via vegetation transpiration and soil evaporation. Thus, enhancement in EF in a warmer environment also implicates the susceptibility of the vegetation present in a measured canopy/land cover to drought conditions.

Earlier studies have established that the EF can be modulated by a range of factors, including vapor pressure deficit (VPD), soil moisture, canopy structure, atmospheric composition, solar radiation and stomatal behaviour [Baldocchi, 1997; Wilson et al., 2002]. VPD, which describes the near surface moisture deficit for a given temperature (difference between the saturated and ambient vapor pressure for atmospheric water) is arguably the dominant nonlinear forcing on EF variability [Gu et al., 2006]. On one hand, an increase in VPD leads to the partitioning of more of the available energy into LH to meet the atmospheric moisture demand, part of the physical control on evapotranspiration [ET; Penman, 1948; Monteith et al., 1965]. On the other hand, high VPD also triggers partial closure of leaf stomata in response to increased atmospheric dryness [Jones and Sutherland, 1991; Damour et al., 2010; Medlyn et al., 2011]. This is part of the physiological control on ET, causing an increase in VPD to actually decrease ET (and thus EF) [Rigden & Salvucci, 2017]. Moreover, the sign of VPD-EF association could also change due to variations in confounding factors like ambient soil moisture and diffuse/direct radiation [Gu et al., 2006]. More diffused radiation enhances plant productivity [Mercado et al., 2009; Rap et al., 2018] and plant growth [Wang et al., 2018]; which, in turn, can increase LH and EF [Davin et al., 2012; Wang et al., 2008]. However, this association is also reported to have an optimum point beyond which plant productivity declines with increasing diffuse fraction [Knohl et al., 2008].

Small particles suspended in the atmosphere, i.e. atmospheric aerosols, can alter the amount of shortwave and longwave radiation reaching the surface, through scattering and absorption, thereby altering NR [Schwartz, 1996; Trenberth et al., 2009; Chakraborty and Lee, 2019]. This is commonly known as the aerosol direct radiative effect (ADRE) and is dependent on aerosol size, composition and vertical distribution in the atmosphere [Forster et al., 2007; Sarangi et al., 2016]. Global and regional scale modelling studies have reported that the ADRE can greatly alter the surface fluxes and microclimate over land [Liu et al., 2014; Mallet et al., 2009; Shen et al., 2020; Myhre et al., 2018]. Generally, the ADRE reduces NR, which results in the reduction in the magnitude of SH and LH. But, loading of scattering aerosols from fossil fuel

https://doi.org/10.5194/acp-2021-40
Preprint. Discussion started: 1 June 2021


Atmospheric Chemistry and Physics Discussions

combustion can also increases the diffuse fraction of solar radiation at the surface, which affects the photosynthesis and LH or EF [Chameides et al., 1999; Matsui et al., 2008;Niyogi et al., 2004; Wang et al., 2008; O'Sullivan et al., 2016; Wang et al., 2020]. This mechanism is generally referred to in the literature as the aerosol diffuse radiation fertilization effect (ADFE). But, depending on the ecosystem, the positive association of ADFE on EF also gets saturated as ADRE becomes larger than a threshold [Yue et al., 2017]. Further, Steiner et al., [2013] reported that warmer air temperature are consistent with high AOD scenario over various in-situ micrometeorological sites in USA, which can result in no clear association between AOD and LH. Thus, how aerosol loading modulates the already complex VPD-EF association can depend on the interplay between radiation, ADFE, aerosol amount and properties, background climate and ecosystem phenology [Steiner et al., 2011].

Northern India is a global hot spot for atmospheric aerosols with aerosol optical depth (AOD) varying between 0.5 and 1.5, and high aerosol radiative efficiency values ( ~100 $W/m^2/AOD$) during pre-monsoon period [Dey et al., 2011; Kumar et al., 2015; Dimitris et al., 2012; Sarangi et al., 2016; Srivastava et al., 2011]. In addition, the region also experiences frequent high temperature days and heatwave conditions, generally extending for 2-6 days during this period [Ratnam et al., 2016; Rohini et al., 2016]. During heatwave conditions, the regional atmosphere is largely stagnant [Ratnam et al., 2016], which can lead to greater air temperature by 5-10 K and magnifies the water vapour demand by 2-3 times at weekly time scale. In addition to high air temperatures ($T_{air}$), high aerosol loading during heatwaves have also been reported over Northern India [Dave et al., 2020; Mondal et al., 2020] at this time of year. Moreover, the value of EF is typically greater than 0.5 over the Northern India during pre-monsoon period, indicating a potentially larger control of VPD-LH linkages on surface energy partitioning [Bhat et al., 2019]. Steep variability in ambient values of VPD (also AOD in some events) during heatwaves over Northern India provides us with ideal conditions for investigating the associations between aerosol loading and VPD-EF coupling.

Previous studies have suggested that aerosol loading can modulate the partitioning of surface fluxes over Northern India [Urankar et al., 2012; Murthy et al., 2014; Latha et al., 2019; Gupta et al., 2020]. However, these studies have been based on reanalysis products [Urankar et al 2012], very limited measurements of SH only [Murthy et al., 2014] or estimated derived from remotely sensed data [Latha et al., 2019] and therefore lack the fidelity that be obtained from direct observations of key processes. Better understanding of the aerosol-VPD-EF associations using direct collocated observations is essential to understand present day conditions and potential feedbacks that can modify future climate over this region of great hydro-climatic significance. In this study, we have used co-located observations of surface energy balance, near-surface micrometeorological variables and soil characteristics, together with aerosol properties (both surface and columnar) at a sub-tropical site in northern India during the pre-monsoon season. Analysis of case studies with AOD varying in phase or remaining constant with high VPD (under heatwave conditions) are done to understand the underlying processes. Here, we will present compelling evidence that changes in EF is directly (indirectly) proportional to aerosol loading (VPD). More interestingly, we found that aerosol loading can decouple the observed strong VPD-LH relationship under heatwave scenario which can have serious implications on climate resilience of crops and vegetation. Below, the sections are organized to discuss the data used, case studies selected and methodology, results, discussions and summary of this study.

https://doi.org/10.5194/acp-2021-40
Preprint. Discussion started: 1 June 2021


Atmospheric Chemistry and Physics Discussions

## 2. Observation site and data:

Observations of SH, LH and net ecosystem $CO_2$ exchange (NEE) were obtained over a semi-natural grassland site (Figure 1A) within the campus of the Indian Institute of Technology, Kanpur (IITK; 26.5N, 80.3E, elevation 132 m above mean sea level) during the pre-monsoon months (April-June) of 2016-2017. Energy flux data were collected by an eddy covariance (EC) system installed at 5.28 m above the soil surface. This flux measurement site is part of an EC network set up in India as part of the INCOMPASS project of the Indo-UK Monsoon Programme [Chakraborty et al., 2019; Turner et al. 2019; Bhat et al., 2019]. The EC system consists of a Windmaster sonic anemometer-thermometer (Gill Instruments Ltd. Lymington, UK) and a LI7500 infrared gas analyzer (LI-COR Biosciences, Logan, Utah, USA). The fetch around the tower is a mixture of different C4 grasses that is representative of grasslands in the region. The vegetation cover is more than 90% of the fetch of the flux tower (Figure 1B) and the canopy height varied within 1-1.5 m during our study periods. The soil is typical of the Gangetic Plains with silt, clay and sand fractions of 80%, 15% and 5%, respectively (unpublished data). The site experiences a humid subtropical climate. The range in daily AOD and $T_{air}$ was 0.4-1.4 and 32-45 $^{O}$C, respectively, during the study period (Figure 1C).

The net radiation (NR; W $m^{-2}$) and its incoming and outgoing short- and longwave components were measured using an NR01 net radiometer (Hukesflux, Delft, The Netherlands) installed at 5 m above the surface. The surface temperature ($T_{srf}$) was calculated from the measured outgoing longwave radiation following the Stefan–Boltzmann law assuming an emissivity of 0.95 [Trenberth et al., 2009]. Soil heat fluxes (GH; W $m^{-2}$) were monitored at 0.03 m below the soil surface using two HFP01-SC self-calibrating soil heat flux plates (Hukesflux, Delft, The Netherlands). Air temperature ($T_{air}$; °C) and relative humidity (RH; %) were measured at a height of 4.5 m. Wind speed and wind direction were measured at 10 m above the soil surface using a WindSonic anemometer (Gill Instruments Ltd., Lymington, UK). Volumetric soil water content (VWC; $m^3$ of water in $m^3$ of soil) and surface temperature ($T_{srf}$; °C) were measured using two pairs of digital TDT sensors (Acclima Inc., Meridian, Idaho, USA) installed at 0.05 and 0.15 m below the soil surface. Standard data processing and quality control routines were used to calculate surface fluxes as described in Morrison et al. 2019. Data gap-filling and the partitioning of NEE into Gross Primary Production (GPP) and total ecosystem respiration was performed using the R EddyProc package [Reichstein et al., 2016; Reichstein et al., 2005]. Negative NEE during the daytime period indicates that photosynthesis at our site dominates over soil and plant respiration (not shown). Since water and carbon cycles in the plants are closely coupled [Collatz et al., 1991]; variations in GPP are used as a proxy for plant transpiration in this study. More details on the flux, weather and radiation tower measurements at IIT Kanpur can be found in Table S1 and Chakraborty et al., 2019.

Version 2 instantaneous cloud screened (Level 1.5) half-hourly averages of AOD (550 nm) and Single Scattering Albedo (SSA), the ratio of scattering efficiency to total extinction efficiency, at 440 nm obtained from the AErosol RObotic NETwork (AERONET) station deployed in the IITK campus (Figure 1A) were used to quantify the aerosol optical properties during our study period. Low and high SSA values indicate dominance of absorbing and scattering aerosols in the column, respectively. Clear-sky SW (0.25–4μm) radiative transfer

https://doi.org/10.5194/acp-2021-40
Preprint. Discussion started: 1 June 2021




calculations, using the Santa Barbara DISORT (discrete ordinates radiative transfer) Atmospheric Radiative Transfer Model (SBDART) [Ricchiazzi et al., 1998], are used to estimate the midday aerosol direct radiative forcing (ADRF) at surface and diffuse radiation reaching the surface ($diffuse_{frac}$). Midday mean AOD and SSA for each day are prescribed to the model. More details on radiative flux calculations using SBDART are mentioned in Supplementary Information file. Finally, micro-pulse lidar backscatter images (Level 1.5) measured at the collocated Micro-Pulse Lidar Network (MPLNET) site [Campbell et al., 2002; Welton and Campbell, 2002] are also used in this study, mainly to identify cloudy days. A day is termed as a cloudy day if cloud patches are observed in MPLNET profiles for more than 3 hours. More details on the aerosol measurements can be found in supplementary information file.

## 3. Case studies and methodology:

The measurements at our site reflect land-atmosphere-energy balance continuum. Thus, in order to examine the impact of aerosols or VPD on EF, we need to carefully identify periods where the variability of other confounding factors is negligible. As such, we identified three weeks (marked in Figure 1C) for analysis, where daily variations in all these factors except $T_{air}$ /VPD and AOD is negligible. Figure 1C illustrates the occurrences of cloudy days, rainfall and wildfire-affected periods during pre-monsoon months of 2016 and 2017. We have avoided periods of cloud and rainfall occurrences since that would affect the surface and energy budget much more than the ADFE. The daily mean VWC values are also shown for the period in Figure 1C. However, as shown in Figure 1C, it is rare to have a considerable time interval with only variation in AOD values (and negligible variation in $T_{air}$/VPD). Hence, three different combinations of $T_{air}$ /VPD and AOD is selected for analysis. The first week selected for analysis is between 2$^{nd}$-9$^{th}$ June, 2016, which had large variation in AOD values is accompanied with insignificant daily variation in $T_{air}$/VPD (hereafter referred as High AOD-Low $T_{air}$ (HALT) case). The second week is during 10$^{th}$-15$^{th}$ April, 2017, which witnessed significant daily increase in aerosol loading as well as $T_{air}$ (hereafter referred to as the High AOD-High $T_{air}$ (HAHT) case). We also selected a third week during 10$^{th}$-15$^{th}$ May, 2017, when daily variation of AOD is relatively low but the variation in $T_{air}$ is high (hereafter referred to as the Low AOD- High $T_{air}$ (LAHT) case). Interestingly, heatwave conditions were prevalent over North India during the HAHT and LAHT weeks, therefore, a wide range of VPD-AOD-EF variation can be sampled. It was also ensured that no rainfall happened during these three weeks so that the variation in VWC is minor compared to significant daily variations in $T_{air}$ and AOD during our study periods. Further, the variations in the vegetation phenology, winds and boundary layer height are found to be minor within each of these three weeks.

The simultaneous midday (1000-1500 LT) variability in AOD, VPD, EF and the other components of the surface radiative balance is analyzed within the HALT and LAHT cases to understand the susceptibility in various variables to changes in AOD and VPD variations, respectively. Further, we analyze the relative variability in HAHT, and compare and contrast the same with the HALT and LAHT cases to understand the effect of combined effect of AOD and VPD variability. Moreover, the differences in canopy resistance and VPD association between HAHT and LAHT weeks is also calculated to examine the impact of aerosol loading on VPD-EF associations under enhanced heat stress. We calculated the daily midday bulk canopy resistances for both HAHT and LAHT cases by inverting the Penmann-Monteith equation using observed values of available energy, VPD, $T_{srf}$ derived from observed $LW_{out}$, psychrometric constant and

https://doi.org/10.5194/acp-2021-40
Preprint. Discussion started: 1 June 2021


Atmospheric Chemistry and Physics Discussions

slope of vapor pressure curve derived from observed surface pressure and $T_{air}$ respectively, and aerodynamic resistance derived from the observed SH and near-surface temperature gradient.

## 4. Results:

During the HALT period, midday AOD values decreased monotonically from ~1.1 on 2$^{nd}$ June,16 to ~ 0.6 on 9$^{th}$ June,16 (Figure 2A). The daily trend in SSA values was negligible, but SSA values are ~0.92 indicating a predominance of scattering aerosols (Figure 2A). Corresponding values of NR at surface increased monotonically by ~50 W/m2 during the same period (Figure 2D). The enhancement in midday NR with decreasing AOD is strongly driven by the reduction in midday incoming shortwave radiation (ISWR) by ~100 W/m$^2$ (Figure 2D). In agreement, ADRF values at surface decreased by ~80 W/m$^2$ and diffuse$_{frac}$ increased by ~0.10 with increase in scattering aerosols from 2$^{nd}$ June to 9$^{th}$ June, 2016 (Figures S1A and S1D). The daily trend in modelled ADRF values are consistent with the daily reduction trend of ISWR during HALT, reinforcing the expectation that negative daily trend in ISWR and NR during HALT was primarily by aerosol-induced radiative changes.

During, HAHT, the midday AOD values increased monotonically from ~0.3 on 10$^{th}$-11$^{th}$ April to ~ 0.8 on 14$^{th}$-15$^{th}$ April (Figure 2B). Corresponding values of NR and ISWR at surface decreased monotonically by ~100 W/m$^2$ and ~200 W/m$^2$, respectively, during the same period (Figure 2E). Similar to HALT, no daily trend was present in SSA values during HAHT and SSA values are ~ 0.9 indicating presence of scattering aerosols (Figure 2B). Similarly, ADRF values at surface (Figure S1B) were also highest on high AOD days (14$^{th}$-15$^{th}$ April; ~150 W/m$^2$) compared to those on low AOD (10$^{th}$-11$^{th}$ April; ~50 W/m$^2$). At the same time, Diffuse$_{frac}$ at the surface (Figures S1E) increased linearly from ~ 0.5 (on 10$^{th}$ April) to ~0.67 on (15$^{th}$ April) during HAHT indicating increase in diffuse solar radiation with aerosol loading.

In contrast, during LAHT case the variation of AOD values between 11$^{th}$ and 15$^{th}$ May,17 is relatively minor from ~0.84 to ~1.2, respectively (Figure 2C). As the increase in AOD is smaller compared to other two cases, corresponding decrease of NR and ISWR values at surface is also smaller in magnitude (~30 W/m$^2$) during this period. Moreover, the midday SSA values during LAHT are lower (~0.8) compared to HALT and HAHT cases indicating presence of more absorbing aerosols in the column (Figure 2C). Interestingly, the ADRF values at surface during LAHT (Figure S1C) were very high, more than double of the same during HALT and HAHT (i.e. ~350 W/m$^2$). This can be explained by the fact that absorbing aerosols (lower SSA values) were relatively dominant during LAHT compared to the other 2 cases. However, no significant daily variability in ADRF and Diffuse$_{frac}$ at the surface (Figures S1F) is observed indicating insignificant aerosol radiative effect at daily scale during LAHT (as also seen in Figure 2F).

As ADRF induces surface cooling, midday $T_{srf}$ values reduced from ~ 35°C during low AOD days to ~30°C during high AOD days in HALT, respectively (Figure 3A). At the same time, the variability in $T_{air}$ values remain more or less constant during HALT. Therefore, the midday variation of temperature difference between $T_{srf}$ and $T_{air}$ ($\Delta T$, calculated as the difference between $T_{srf}$ and $T_{air}$) is inversely proportionally with aerosol loading for HALT (Figure 3A). Greater the value of $\Delta T$, greater will be the turbulent and convection flux and greater is the tendency of SH flux release at surface. Consequently, SH is also inversely proportional to increase in AOD (and ADRF). With increase (decrease) in $\Delta T$ (AOD) values, the corresponding

https://doi.org/10.5194/acp-2021-40
Preprint. Discussion started: 1 June 2021




SH values increased linearly from ~60 W/m$^2$ on 2$^{nd}$ June till ~ 120 W/m$^2$ by 9$^{th}$ June,16 during HALT (Figure 3D).

By contrast, a distinct and steep increase in daily $T_{air}$ (~10 $^oC$) is seen during HAHT and LAHT cases. Further, the mid-day $T_{srf}$ variability is seen to be increasing in close coupling with the corresponding $T_{air}$ variability during these two cases (Figures 3B-C). This coupling is mainly because of the coexisting stagnant scenario under heatwave periods. Nonetheless, daily ΔT variation is inversely proportional to AOD variation during both the weeks (Figure 3B-C). Because, some portion of the enhancement in $T_{srf}$ is compensated by the ADRF-induced surface cooling during midday, steeper ADRF trend means greater ΔT magnitude. For instance, as ADRF variation is relatively smaller across the week during LAHT compared to that during HAHT, a relatively larger decrease in daily ΔT by > 2 $^oC$ (Figure 3B) is observed during HAHT. Consistently, the magnitude of SH also significantly decreased across the week in HAHT and LAHT. Specifically, the mean values of SH decreased linearly from ~200 W/m$^2$ on 10$^{th}$ April (low AOD) to ~ 100 W/m$^2$ on 15$^{th}$ April (high AOD) during HAHT (Figure 3E). During LAHT, the midday mean SH decreased linearly from ~200 W/m$^2$ on 11$^{th}$ May to ~ 125 W/m$^2$ on 14-15$^{th}$ May, 2017 (Figure 3F).

The midday LH values decreases by ~150 Wm$^{-2}$ from high AOD days to low AOD days during HALT (Figure 3D). However, the increase in LH values with increase in AOD from 10$^{th}$ April,17 to 15$^{th}$ April,17 (HAHT case) is much gradual i.e. ~25 W/m$^{-2}$ (Figure 3E). Specifically, the gradient of LH against AOD is 70 W/m$^2$/AOD and 10 W/m$^2$/AOD for HALT and HAHT cases, respectively. As, VPD values increase steeply in HAHT case (Figure 3H), but no distinct variation in VPD was evident for HALT case (Figure 3G). Keeping in mind that the magnitude of AOD variation in both the cases is similar, the differences in LH gradient with AOD (lower value during HAHT) could be induced by AOD-VPD-LH nonlinear linkages in HAHT. Examination of corresponding midday values of GPP (Figures 3G-F) also illustrate daily variations similar in sign to corresponding LH flux indicating that the daily variation in LH in both the cases is mainly due to associated variation in evapotranspiration.

VPD-associated decline in GPP and thus LH fluxes is even more clearly observed in LAHT case. A strong negative trend in midday values of LH and GPP is observed as the week progressed from low to high VPD during LAHT (Figure 3F and 3I). Quantitatively, the gradient of LH against $T_{air}$ is +4.1 W/m$^2$/$^oC$ and -6.6 W/m$^2$/ $^oC$ for HALT and LAHT cases, respectively. Again, note that the magnitude of VPD variation in both the cases is similar, so the differences in LH-$T_{air}$ can be inferred to be primarily induced by relatively differences in aerosol loading. Thus, changes in magnitude of LH or GPP is proportional to changes in magnitude of AOD, but the same is inversely proportional to variations in $T_{air}$/VPD, and the relative effects can largely compensate each other.

It is interesting to note that variation in EF was only seen in cases where there was an associated variation in AOD. Partitioning of surface energy into LH (LHF; LH/NR) increased and SHF (SH/NR) decreased with increase in AOD during HALT (Figure 3J). As a result, the midday EF distribution decreased with reduction in AOD from ~0.8 on 2$^{nd}$ June to ~0.6 on 9$^{th}$ June during HALT (Figure 3J). Similarly, EF also increased from ~0.63 on 10$^{th}$ April, 2017 to

https://doi.org/10.5194/acp-2021-40
Preprint. Discussion started: 1 June 2021




~0.78 on 15th April, 2017 (Figure 3K) during HAHT due to simultaneous decrease and increase in SHF and LHF at the same time, respectively. However, no substantial variation was observed in EF across the week during LAHT case (Figure 3L). The decrease in SHF with VPD was similar in HAHT and LAHT cases. But, LHF increased (decreased) with VPD during the former (later) case indicating role of AOD on LH-VPD pathways.

Figure 4 illustrates that the canopy resistance increases steeply from 400 to 1400 s $m^{-1}$ with increase in VPD from 40 to 70 hPa during LAHT case. However, the canopy resistance increases from 400 to 500 with increase in VPD from 45 to 65 hPa during HAHT case. The LAHT case illustrates the frequently reported behaviour of reduction of canopy conductance under increase in VPD due to partial stomata closure as a physiological stress response. Interestingly, the comparison of LAHT and HAHT scatter illustrates that canopy conductance is not much affected even under severe VPD rise when aerosol loading also increases in phase. This may indicate that under high aerosol loading vegetation gets relatively decoupled from the physiological stress of VPD increase. This can partially explain the aerosol-induced increase in EF (as well as LH and GPP) even under high VPD rise during HAHT.

## 5. Discussion:

The increase in scattering aerosols increased $Diffuse_{frac}$ during HALT; thereby facilitating relatively more photosynthesis and thus more GPP and LH with increase in AOD. At the same time, increase in AOD also decreased $\Delta T$ and constrained SH release, eventually leading to aerosol-induced increase in EF during HALT. However, previous studies investigating the role of aerosols on surface energy fluxes over India have largely reported that aerosol loading is inversely related to LH or LHF [Murty et al., 2014; Latha et al., 2019; Gupta et al., 2020]. Possible explanations for this apparent contradiction are as follows. First, these studies did not explicitly account for the effect of daily meteorology/ VPD/ temperature variability in their analysis which can have confounding effects (as shown here and discussed in Steiner et al., 2013). Second, these studies were not focused on grassland. Murty et al., 2014 used micrometeorological site data with a forested footprint in Ranchi. At the same time, Latha et al., 2019 performs analysis at 100 km spatial resolution from reanalysis product/Model, which is representative of a composite land use (including cities, forest, cropland and grassland) and thus a mixture of evapotranspiration and ground evaporation. Gupta et al., 2020 used micrometeorological observations within a typical university canopy (buildings, roads and trees) in Mumbai. Nonetheless, our finding of direct proportionality between aerosol loading and LH (or photosynthesis) is consistent with previously reported in-situ studies over grasslands sites in USA [Niyogi et al., 2004; Gu et al., 2002; Wang et al., 2008].

In contrast, aerosol loading and heatwave conditions both reduced SH. Greater ADRE values induces more surface cooling (Chakraborty and Lee, 2019), and hence could lower SH fluxes (Yu et al., 2002; Urankar et al., 2012; Steiner et al., 2013), which is also seen in HALT case. Simultaneously, sensible heat release is also directly proportional to $\Delta T$ near surface during Pre-monsoon (Rao et al., 2019), which is illustrated in LAHT case. In HAHT case, both the effects work in phase to reduce SH. The reduction of SH per unit change of $T_{air}$ is 8 $W/m^2/^oC$ during LAHT compared to the same being 11 $W/m^2/^oC$ in HAHT case. At the same time, the

https://doi.org/10.5194/acp-2021-40
Preprint. Discussion started: 1 June 2021



reduction of SH per unit change of AOD is 135 W/m$^2$/AOD during LAHT compared to the same being 65 W/m$^2$/AOD in HALT case. Hence, increase in AOD and $T_{air}$, both suppress the release of available surface energy via SH and the effect is largely additive. Moreover, the intensity of the AOD-induced SH suppression will be stronger if the aerosols are composed of relatively more absorbing aerosols, specifically black carbon [Myhre et al., 2018]. Because, they not only cools the $T_{srf}$ (Mallet et al., 2009; Pandithurai et al., 2008a; Shen et al., 2020) but also can warm $T_{air}$ (especially under stagnant/heatwave conditions), thereby reducing $\Delta T$ and inducing lower tropospheric stability [Dave et al., 2020; Steiner et al., 2013; Myhre et al., 2018].

However, contrary to our results, a recent modelling study over India reports that enhancement of absorbing aerosols under heatwave scenario causes increase in SH along with air temperature [Mondal et al., 2020]. The inherent model biases in the aerosol properties and concentration as well as absence of detailed aerosol-plant-atmosphere processes in the model simulations of Mondal et al., 2020 may cause differences in the signature of the AOD-SH feedback. At the same time, the above differences can also be explained by taking into consideration the difference in time-scale of the feedback used in analysis. For example, a robust positive association between morning time black carbon concentrations and mid-day $T_{air}$ is observed by Talukdar et al., 2020. Although, they attributed this association primarily to diurnality in residual layer mixing, our understanding here can also explain a possible pathway. High black carbon loading during morning time can suppress instantaneous SH release (via reduction in the $\Delta T$), followed by release of the additional SH amount in the mid-day period under relatively unstable atmosphere (and lower black carbon concentration due to dilution effect). As such, correlations between absorbing aerosols and SH at instantaneous scale can be negative (as seen in HAHT), but correlations at daily or monthly time scale may involve feedbacks which can result in positive associations (as also seen in Mondal et al., 2020).

In addition, our results clearly suggest the complexity and non-linearity between aerosol, VPD and EF, and provides observational evidence to the discussions reported in Steiner et al., 2011; 2013. Keeping all other factors relatively constant, increase in scattering aerosols causes a positive AOD-EF association (as seen in HALT). In case of HAHT, as both AOD and VPD increased in phase over the week, VPD-induced reduction in LH compensated a major portion of the $Diffuse_{frac}$-induced increase in LH resulting in a net increase in LHF with increase in AOD. Also note that, combined effect of increase in AOD and $T_{air}$ caused a large decrease in SHF. Thus, EF also increases with AOD under heatwave conditions. However, in absence of significant aerosol variation, the increase in VPD causes a large reduction in LH and LHF (as seen in LAHT). First, negligible ADFE and second, increase in canopy resistance (via stomatal aperture reduction) under steep rise in VPD values can explain the large reduction in LHF during LAHT. High VPD is also linked with greater $T_{air}$ during heatwave scenarios, thereby inducing reduction in $\Delta T$ and SHF during LAHT. Thus, both SHF and LHF decreased with VPD causing an increase in midday ground heat flux during heatwave events and negligible change in EF with VPD. Moreover, the increase in ground heat flux results in an increase in $T_{srf}$ (as seen in HAHT and LAHT cases) thereby feeding the reduction in $\Delta T$ and SHF in the first place. Thus, the VPD-EF coupling is very strong in absence of aerosol loading but weakens when aerosol increases.

India's mean temperature has already increased by ~ 0.7 degree Celsius since 1900 and is projected to rise by ~4.5 degree Celsius by the end of 2100 relative to present day scenario

https://doi.org/10.5194/acp-2021-40
Preprint. Discussion started: 1 June 2021



[Krishnan et al., 2020]. At the same time, the global mean VPD is increasing with global warming [Yuan et al., 2019] and heatwaves will be more frequent in future India [Mukherjee et al., 2018]. Moreover, anthropogenic emissions over Indian Subcontinent will ensure high AOD values in near future [Kumar et al 2018], thus manifesting a HAHT scenario in future India. In this context, our finding that aerosols can reduce the VPD-induced physiological stress on vegetation can have substantial implications. Although, the exact pathway is still not clear, the phenomena of aerosol-induced weakening of the physiological-response by vegetation can make plants and trees less heat-resilient in future. While ADFE can be a potential pathway of aerosol-induced VPD-EF decoupling, possible physiological changes in stomata aperture due to direct deposition of aerosols as a wax layer can also contribute [Burkhardt., 2010; Burkhardt and Grantz., 2017]. Recently, Grantz *et al*. 2018 used direct observations in glasshouses to illustrate similar uncoupling of stomata conductance (flux-based) from its porosity (higher VPD induces reduction in pore size) under more aerosol scenario. Nonetheless, the sensitivity and sign of the AOD-VPD-EF associations depends on the region-specific physiological feedback of vegetation, ambient aerosol optical properties, vegetation structure and VWC. Therefore, land process models should be well-constrained with better quantification of aerosol-$T_{air}$-VPD-EF continuum for accurately projecting future regional climate, crop yield and adaptation strategies.

## 6. Summary

In summary, simultaneous measurements from AERONET and an eddy covariance flux tower equipped with micrometeorological and soil physics sensors were employed to understand aerosol-Evaporative fraction associations and their variability with meteorology over a natural C4 grassland site under clear sky conditions in the central Gangetic Plains. The main findings from this study are:

1. Increase in aerosol loading reduces the incoming solar radiation at surface and reduces the gradient between surface temperature and near-surface air temperature. This is associated with the decrease in energy dissipation from surface via SH. At the same time, increase in aerosol loading increases the evapotranspiration efficiency of ecosystem by increasing diffuse radiation. Thus, high aerosol loading favors dissipation of available surface energy via Latent heat flux and therefore increases Evaporative fraction.
2. Increase in surface temperature and VPD during heatwave conditions induce larger canopy resistance and stomata closure, thereby reducing the LH fluxes and EF. Plants tend to store more water by transpiring less in high temperature conditions; so GPP (and thus LH) reduces under high temperatures. At the same time, higher air temperature, also reduces the SH via lower $\Delta T$. Thus, as the effect of VPD involves reducing both SH and LH, the net effect on EF is negligible.
3. The variability in aerosol loading plays a significant role in modulating the VPD-EF association under varying VPD/surface temperature. When the changes in VPD and scattering aerosols are in phase, like in case of heat wave conditions over North India, the VPD-induced reduction in LH may be completely compensated by the enhancement in LH via ADFE or physiological changes due to aerosol coating on leaves. Moreover, as both increasing AOD and $T_{air}$ induces reduction in SH, the changes in net EF under such conditions is also in phase with AOD and VPD.

To sum up, the observational evidence provided in this study not only encourages more measurements and mechanistic experiments of aerosol-plant-atmosphere interactions, but also warrants proper representations of aerosol physical and physiological properties in land process models over this region of strong aerosol-land-atmosphere coupling.

**Acknowledgement:**
SNT gratefully acknowledge the financial support given by the Earth System Science Organization, Ministry of Earth Sciences, Government of India (grant MM/NERC-MoES-03/2014/002) and Newton Fund to conduct this research under Monsoon Mission. LMM acknowledges the support of the Natural Environment Research Council (NERC) South AMerican Biomass Burning Analysis (SAMBBA) project grant code NE/J010057/1. The authors would like to thank Dr E. J. Welton, B.N. Holben and staff at NASA GSFC for establishing and quality control of the AERONET and MPLNET site at IIT Kanpur, used in this study.

**Data statement:**
Surface data used here is available at: https://catalogue.ceh.ac.uk/documents/78c64025-1f8d-431c-bdeb-e69a5877d2ed. Aerosol data used here is available from https://www.iitk.ac.in/ce/aeronet.

**References**

1. Bollasina, M. A., and Y. Ming (2013), The role of land-surface processes in modulating the Indian monsoon annual cycle, Climate Dynamics, 41(9-10), 2497-2509.
2. Campbell, J. R., D. L. Hlavka, E. J. Welton, C. J. Flynn, D. D. Turner, J. D. Spinhirne, V. S. S. III, and I. H. Hwang (2002), Full-Time, Eye-Safe Cloud and Aerosol Lidar Observation at Atmospheric Radiation Measurement Program Sites: Instruments and Data Processing, Journal of Atmospheric and Oceanic Technology, 19(4), 431-442.
3. Chakraborty, S., U. Saha, and A. Maitra (2015), Relationship of convective precipitation with atmospheric heat flux — A regression approach over an Indian tropical location, Atmospheric Research, 161–162, 116-124.
4. Chameides, W. L., et al. (1999), Case study of the effects of atmospheric aerosols and regional haze on agriculture: An opportunity to enhance crop yields in China through emission controls?, Proceedings of the National Academy of Sciences, 96(24), 13626-13633.
5. Collatz, G. J., J. T. Ball, C. Grivet, and J. A. Berry (1991), Physiological and environmental regulation of stomatal conductance, photosynthesis and transpiration: a model that includes a laminar boundary layer, Agricultural and Forest Meteorology, 54(2), 107-136.
6. Dey, S., and L. Di Girolamo (2011), A decade of change in aerosol properties over the Indian subcontinent, Geophysical Research Letters, 38(14), n/a-n/a.
7. Dimitris, G. K., P. S. Ramesh, G. Ritesh, S. Manish, P. G. Kosmopoulos, and S. N. Tripathi (2012), Variability and trends of aerosol properties over Kanpur, northern India using AERONET data (2001–10), Environmental Research Letters, 7(2), 024003.
8. Forster, P., V. Ramaswamy, P. Artaxo, T. Berntsen, R. Betts, D. W. Fahey, J. Haywood, J. Lean, D. C. Lowe, and G. Myhre (2007), Changes in atmospheric constituents and in radiative forcing. Chapter 2, in Climate Change 2007. The Physical Science Basis, edited.

https://doi.org/10.5194/acp-2021-40
Preprint. Discussion started: 1 June 2021



9. Gautam, R., N. C. Hsu, and K. M. Lau (2010), Premonsoon aerosol characterization and radiative effects over the Indo-Gangetic Plains: Implications for regional climate warming, Journal of Geophysical Research: Atmospheres, 115(D17), n/a-n/a.
10. Gautam, R., et al. (2011), Accumulation of aerosols over the Indo-Gangetic plains and southern slopes of the Himalayas: distribution, properties and radiative effects during the 2009 pre-monsoon season, Atmos. Chem. Phys., 11(24), 12841-12863.
11. Gu, L., T. Meyers, S. G. Pallardy, P. J. Hanson, B. Yang, M. Heuer, K. P. Hosman, J. S. Riggs, D. Sluss, and S. D. Wullschleger (2006), Direct and indirect effects of atmospheric conditions and soil moisture on surface energy partitioning revealed by a prolonged drought at a temperate forest site, Journal of Geophysical Research: Atmospheres, 111(D16), n/a-n/a.
12. Jones, H. G., and R. A. Sutherland (1991), Stomatal control of xylem embolism, Plant, Cell & Environment, 14(6), 607-612.
13. Liu, S., M. Chen, and Q. Zhuang (2014), Aerosol effects on global land surface energy fluxes during 2003–2010, Geophysical Research Letters, 41(22), 7875-7881.
14. Mallet, M., P. Tulet, D. Serça, F. Solmon, O. Dubovik, J. Pelon, V. Pont, and O. Thouron (2009), Impact of dust aerosols on the radiative budget, surface heat fluxes, heating rate profiles and convective activity over West Africa during March 2006, Atmos. Chem. Phys., 9(18), 7143-7160.
15. Matsui, T., A. Beltrán-Przekurat, D. Niyogi, R. A. Pielke, and M. Coughenour (2008), Aerosol light scattering effect on terrestrial plant productivity and energy fluxes over the eastern United States, Journal of Geophysical Research: Atmospheres, 113(D14), n/a-n/a.
16. Murthy, B. S., R. Latha, K. Manoj, and N. C. Mahanti (2014), Effect of aerosols on evapo-transpiration, Atmospheric Environment, 89, 109-118.
17. Niyogi, D., H.-I. Chang, F. Chen, L. Gu, A. Kumar, S. Menon, and R. A. Pielke (2007), Potential impacts of aerosol–land–atmosphere interactions on the Indian monsoonal rainfall characteristics, Natural Hazards, 42(2), 345-359.
18. Niyogi, D., et al. (2004), Direct observations of the effects of aerosol loading on net ecosystem CO2 exchanges over different landscapes, Geophysical Research Letters, 31(20), n/a-n/a.
19. Pandithurai, G., C. Seethala, B. S. Murthy, and P. C. S. Devara (2008a), Investigation of atmospheric boundary layer characteristics for different aerosol absorptions: Case studies using CAPS model, Atmospheric Environment, 42(19), 4755-4768.
20. Pandithurai, G., S. Dipu, K. K. Dani, S. Tiwari, D. S. Bisht, P. C. S. Devara, and R. T. Pinker (2008b), Aerosol radiative forcing during dust events over New Delhi, India, Journal of Geophysical Research: Atmospheres, 113(D13), n/a-n/a.
21. Saha, S. K., S. Halder, K. K. Kumar, and B. N. Goswami (2011), Pre-onset land surface processes and 'internal' interannual variabilities of the Indian summer monsoon, Climate Dynamics, 36(11), 2077-2089.
22. Sarangi, C., S. N. Tripathi, A. K. Mishra, A. Goel, and E. J. Welton (2016), Elevated aerosol layers and their radiative impact over Kanpur during monsoon onset period, Journal of Geophysical Research: Atmospheres, 121(13), 7936-7957.
23. Schwartz, S. E. (1996), Atmospheric AerosolsThe whitehouse effect—Shortwave radiative forcing of climate by anthropogenic aerosols: an overview, Journal of Aerosol Science, 27(3), 359-382.

https://doi.org/10.5194/acp-2021-40
Preprint. Discussion started: 1 June 2021


Atmospheric Chemistry and Physics
Discussions


24. Srivastava, A., S. Tiwari, P. Devara, D. Bisht, M. K. Srivastava, S. Tripathi, P. Goloub, and B. Holben (2011), Pre-monsoon aerosol characteristics over the Indo-Gangetic Basin: implications to climatic impact, paper presented at Annales Geophysicae, European Geosciences Union.
25. Steiner, A. L., and W. L. Chameides (2011), Aerosol-induced thermal effects increase modelled terrestrial photosynthesis and transpiration, Tellus B, 57(5).
26. Steiner, A. L., D. Mermelstein, S. J. Cheng, T. E. Twine, and A. Oliphant (2013), Observed Impact of Atmospheric Aerosols on the Surface Energy Budget, Earth Interactions, 17(14), 1-22.
27. Trenberth, K. E., J. T. Fasullo, and J. Kiehl (2009), Earth's Global Energy Budget, Bulletin of the American Meteorological Society, 90(3), 311-323.
28. Urankar, G., T. V. Prabha, G. Pandithurai, P. Pallavi, D. Achuthavarier, and B. N. Goswami (2012), Aerosol and cloud feedbacks on surface energy balance over selected regions of the Indian subcontinent, Journal of Geophysical Research: Atmospheres, 117(D4), n/a-n/a.
29. Wang, K., and R. E. Dickinson (2012), A review of global terrestrial evapotranspiration: Observation, modeling, climatology, and climatic variability, Reviews of Geophysics, 50(2), n/a-n/a.
30. Wang, K., R. E. Dickinson, and S. Liang (2008), Observational evidence on the effects of clouds and aerosols on net ecosystem exchange and evapotranspiration, Geophysical Research Letters, 35(10), n/a-n/a.
31. Welton, E. J., and J. R. Campbell (2002), Micropulse Lidar Signals: Uncertainty Analysis, Journal of Atmospheric and Oceanic Technology, 19(12), 2089-2094.
32. Yu, H., S. C. Liu, and R. E. Dickinson (2002), Radiative effects of aerosols on the evolution of the atmospheric boundary layer, Journal of Geophysical Research: Atmospheres, 107(D12), AAC 3-1-AAC 3-14.
33. Koster, R. D., Dirmeyer, P. A., Guo, Z., Bonan, G., Chan, E., Cox, P., ... & Liu, P. (2004). Regions of strong coupling between soil moisture and precipitation. *Science*, *305*(5687), 1138-1140.
34. Turner, A. G., Bhat, G. S., Martin, G. M., Parker, D. J., Taylor, C. M., Mitra, A. K., ... & Morrison, R. (2019). Interaction of convective organization with monsoon precipitation, atmosphere, surface and sea: The 2016 INCOMPASS field campaign in India. *Quarterly Journal of the Royal Meteorological Society*.
35. Chakraborty, T., & Lee, X. (2019). Land cover regulates the spatial variability of temperature response to the direct radiative effect of aerosols. *Geophysical Research Letters*, *46*(15), 8995-9003.
36. Chakraborty, T., Sarangi, C., Krishnan, M., Tripathi, S. N., Morrison, R., & Evans, J. (2019). Biases in model-simulated surface energy fluxes during the Indian monsoon onset period. *Boundary-Layer Meteorology*, *170*(2), 323-348.

37. Rigden, A. J., & Salvucci, G. D. (2017). Stomatal response to humidity and CO 2 implicated in recent decline in US evaporation. *Global Change Biology*, *23*(3), 1140-1151.
38. Yuan, W., Zheng, Y., Piao, S., Ciais, P., Lombardozzi, D., Wang, Y., ... & Jain, A. K. (2019). Increased atmospheric vapor pressure deficit reduces global vegetation growth. *Science advances*, *5*(8), eaax1396.

https://doi.org/10.5194/acp-2021-40
Preprint. Discussion started: 1 June 2021

Atmospheric Chemistry and Physics Discussions


39. Wang Z., C. Wang, B. Wang, X. Wang, J. Li, J. Wu, L. Liu Interactive effects of air pollutants and atmospheric moisture stress on aspen growth and photosynthesis along an urban-rural gradient. Environ. Pollut., 260 (2020), Article 114076, 10.1016/j.envpol.2020.114076
40. Burkhardt J, Grantz DA. 2017. Plants and atmospheric aerosols. Progress Botany 78: 369–406
41. Burkhardt J. 2010. Hygroscopic particles on leaves: nutrients or desiccants? *Ecological Monographs* **80**: 369– 399.
42. Grantz DA, Zinsmeister D, Burkhardt J. 2018. Ambient aerosol increases minimum leaf conductance and alters the aperture–flux relationship as stomata respond to vapor pressure deficit (VPD). *New Phytologist* **219**: 275– 286.
43. R. Latha, B. S. Murthy & B. Vinayak (2019) Aerosol-induced perturbation of surface fluxes over different landscapes in a tropical region, International Journal of Remote Sensing, 40:21, 8203-8221, DOI: 10.1080/01431161.2018.1523586
44. Krishnan et al (2020) Assessment of climate change over the Indian region: a report of the Ministry of Earth Sciences (MoES), Government of India
45. WangX., J. Wu, M. Chen, X. Xu, Z. Wang, B. Wang, C. Wang, S. Piao, W. Lin, G. Miao, Deng, C. Qiao, J. Wang, S. Xu, L. Liu, Field evidences for the positive effects of aerosols on tree growth. Global Change Biol., 24 (2018), pp. 4983-4992
46. Myhre, G., Samset, B.H., Hodnebrog, Ø. *et al.* Sensible heat has significantly affected the global hydrological cycle over the historical period. *Nat Commun* **9,** 1922 (2018). https://doi.org/10.1038/s41467-018-04307-4
47. Rao, K. G., & Reddy, N. N. (2019). On moisture flux of the Indian summer monsoon: A new perspective. *Geophysical Research Letters*, 46, 1794– 1804. https://doi.org/10.1029/2018GL080392
48. Mondal, A, Sah, N, Sharma, A, Venkataraman, C, Patil, N. Absorbing aerosols and high-temperature extremes in India: A general circulation modelling study. *Int J Climatology*. 2020; 1– 20. https://doi.org/10.1002/joc.6783
49. Shen Z, Ming Y, Held IM. Using the fast impact of anthropogenic aerosols on regional land temperature to constrain aerosol forcing. Sci Adv. 2020 Aug 5;6(32): doi: 10.1126/sciadv.5297.
50. Dave P, Bhushan, M., Venkatraman, C., Absorbing aerosol influence on temperature maxima: An observation-based study over India. Atmospheric Environment, Volume 223, 2020, 117237, ISSN 1352-2310, https://doi.org/10.1016/j.atmosenv.2019.117237.
51. Talukdar S. and M.V. Ratnam, A mutual response between surface temperature and black carbon mass concentration during the daytime, Science of the Total Environment, https://doi.org/10.1016/j.scitotenv.2020.143477
52. Knohl, A., and D. D. Baldocchi (2008), Effects of diffuse radiation on canopy gas exchange processes in a forestecosystem, J. Geophys. Res., 113, G02023, doi:10.1029/2007JG000663
53. Davin, E. L. and Seneviratne, S. I.: Role of land surface processes and diffuse/direct radiation partitioning in simulating the European climate, Biogeosciences, 9, 1695–1707, https://doi.org/10.5194/bg-9-1695-2012, 2012
54. O'Sullivan, M., A. Rap, C. L. Reddington,D. V. Spracklen, M. Gloor, andW. Buermann (2016), Small global effecton terrestrial net primary productiondue to increased fossil fuel

aerosol emissions from East Asia since the turnof the century, Geophys. Res. Lett., 43,8060–8067, doi:10.1002/2016GL068965.

55. Yue, X. and Unger, N.: Aerosol optical depth thresholds as a tool to assess diffuse radiation fertilization of the land carbon uptake in China, Atmos. Chem. Phys., 17, 1329–1342, https://doi.org/10.5194/acp-17-1329-2017, 2017.
56. Mercado LM, Bellouin N, Sitch S, Boucher O, Huntingford C, Wild M, Cox PM. Impact of changes in diffuse radiation on the global land carbon sink. Nature. 2009 Apr 23;458(7241):1014-7. doi: 10.1038/nature07949. PMID: 19396143.
57. Kumar, R., Barth, M. C., Pfister, G. G., Delle Monache, L., Lamarque, J. F., Archer-Nicholls, S.,Walters, S. (2018). How will air quality change in South Asia by 2050? *Journal of Geophysical Research: Atmospheres*, 123, 1840– 1864. https://doi.org/10.1002/2017JD027357
58. M. Kumar, K.S. Parmar, D.B. Kumar, A.Mhawish, D.M. Broday, R.K. Mall, T. Banerjee Long-term aerosol climatology over Indo-Gangetic Plain: trend, prediction and potential source field; Atmos. Environ., 180 (2018), pp. 37-50
59. Bhat G. S., R. Morrison, C. M. Taylor, B. K. Bhattacharya, S. Paler,D. Desai,J. G. Evans,S. Pattnaik, M. Sekhar, R. Nigam, A. Sattar, S. S. Angadi, D. Kacha, A. Patidar, S. N. Tripathi, K. V. M. Krishnan, A. Sisodiya; Spatial and temporal variability in energy and water vapour fluxes observed at seven sites on the Indian subcontinent during 2017. *Q J R Meteorol Soc*. 2020; 146: 2853– 2866. https://doi.org/10.1002/qj.3688
60. Ratnam, J., Behera, S., Ratna, S. *et al.* Anatomy of Indian heatwaves. *Sci Rep* 6, 24395 (2016). https://doi.org/10.1038/srep24395.
61. Mukherjee, S., Mishra, V. A sixfold rise in concurrent day and night-time heatwaves in India under 2 °C warming. *Sci Rep* **8,** 16922 (2018). https://doi.org/10.1038/s41598-018-35348-w
62. Morrison, R.; Angadi, S.S.; Cooper, H.M.; Evans, J.G.; Rees, G.; Sekhar, M.; Taylor, C.; Tripathi, S.N.; Turner, A.G. (2019). Energy and carbon dioxide fluxes, meteorology and soil physics observed at INCOMPASS land surface stations in India, 2016 to 2017. NERC Environmental Information Data Centre. https://doi.org/10.5285/78c64025-1f8d-431c-bdeb-e69a5877d2ed
63. Mayank Gupta et al 2021 Environ. Res. Lett. 16 014021
64. Rohini, P., Rajeevan, M. & Srivastava, A. On the Variability and Increasing Trends of Heat Waves over India. *Sci Rep* **6,** 26153 (2016). https://doi.org/10.1038/srep26153

https://doi.org/10.5194/acp-2021-40
Preprint. Discussion started: 1 June 2021


Atmospheric Chemistry and Physics
Open Access
EGU
Discussions

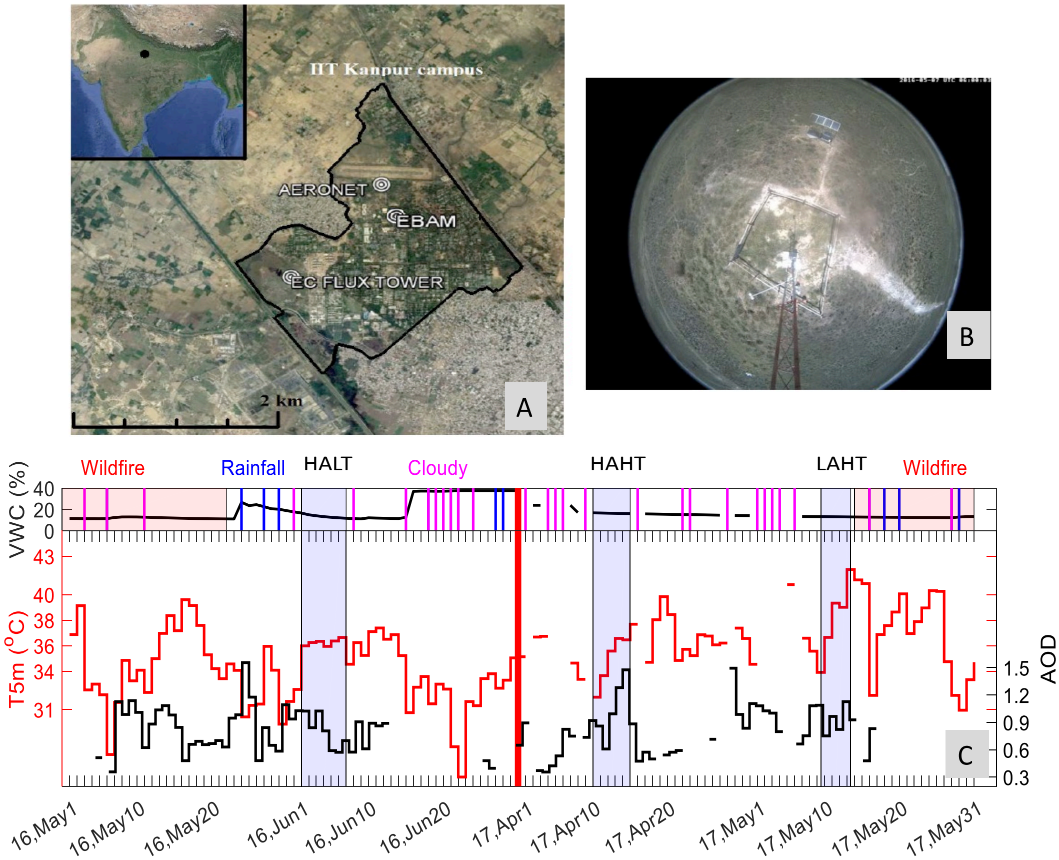


*Figure 1: A) Map showing the locations of AERONET and the EC flux tower site within the campus of the Indian Institute of Technology Kanpur (IITK). Inset map shows the location of IITK (black dot) in the central Gangetic Plains. The maps are created by © Google Maps 2017. B) Camera image of land cover of the flux tower site during May 12th, 2017. C) Daily variation in VWC during our study period is shown in black line in upper box of the figure. The occurrences of cloudy days, rainy days and wildfire affected period during April through June of 2016 and 2017 is shown by magenta, blue and pick colr patches in the upper box. A cloudy day is inferred from MPLNET images and AERONET observations (as defined in Section 2 of main text). The days bounded by straight lines depict the study episodes HALT, HAHT and LAHT, respectively. Daily variation in $T_{air}$ and daily variation in AOD during our study period is shown as black and red lines in lower box of the panel).*

https://doi.org/10.5194/acp-2021-40
Preprint. Discussion started: 1 June 2021


Atmospheric Chemistry and Physics Discussions
Open Access

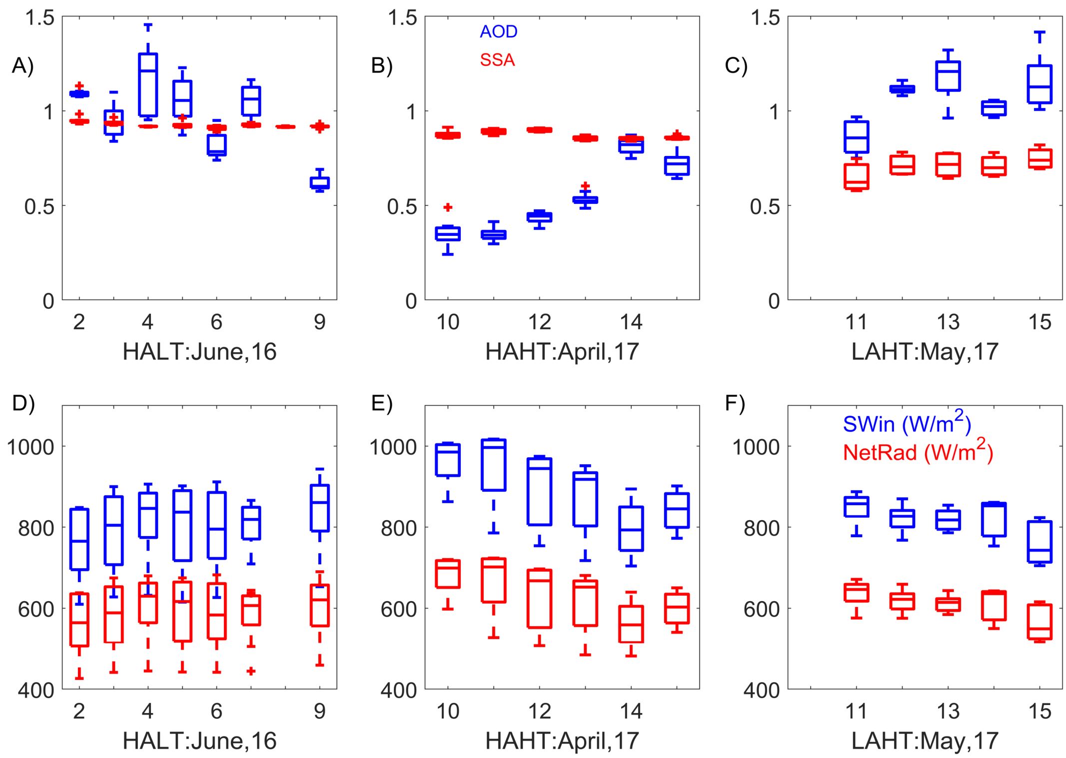


*Figure 2: Box plots showing the variations in aerosol and radiation during the cases. Row 1 illustrates Time series of midday (1100-1400 LT) variation in AOD and SSA values during HALT, HAHT and LAHT, respectively.. The horizontal line within box represents median of the distribution. The bottom and top edge of the boxes represent 25th and 75th percentile, respectively, of the distribution. The short dash at top and bottom extent of the boxes represent 5th and 95th percentile, respectively. Row 2 is same as Row 1 but show measurements of incoming short wave radiation and net radiation at surface. Note that June,16 means June of 2016 and so on.*

https://doi.org/10.5194/acp-2021-40
Preprint. Discussion started: 1 June 2021




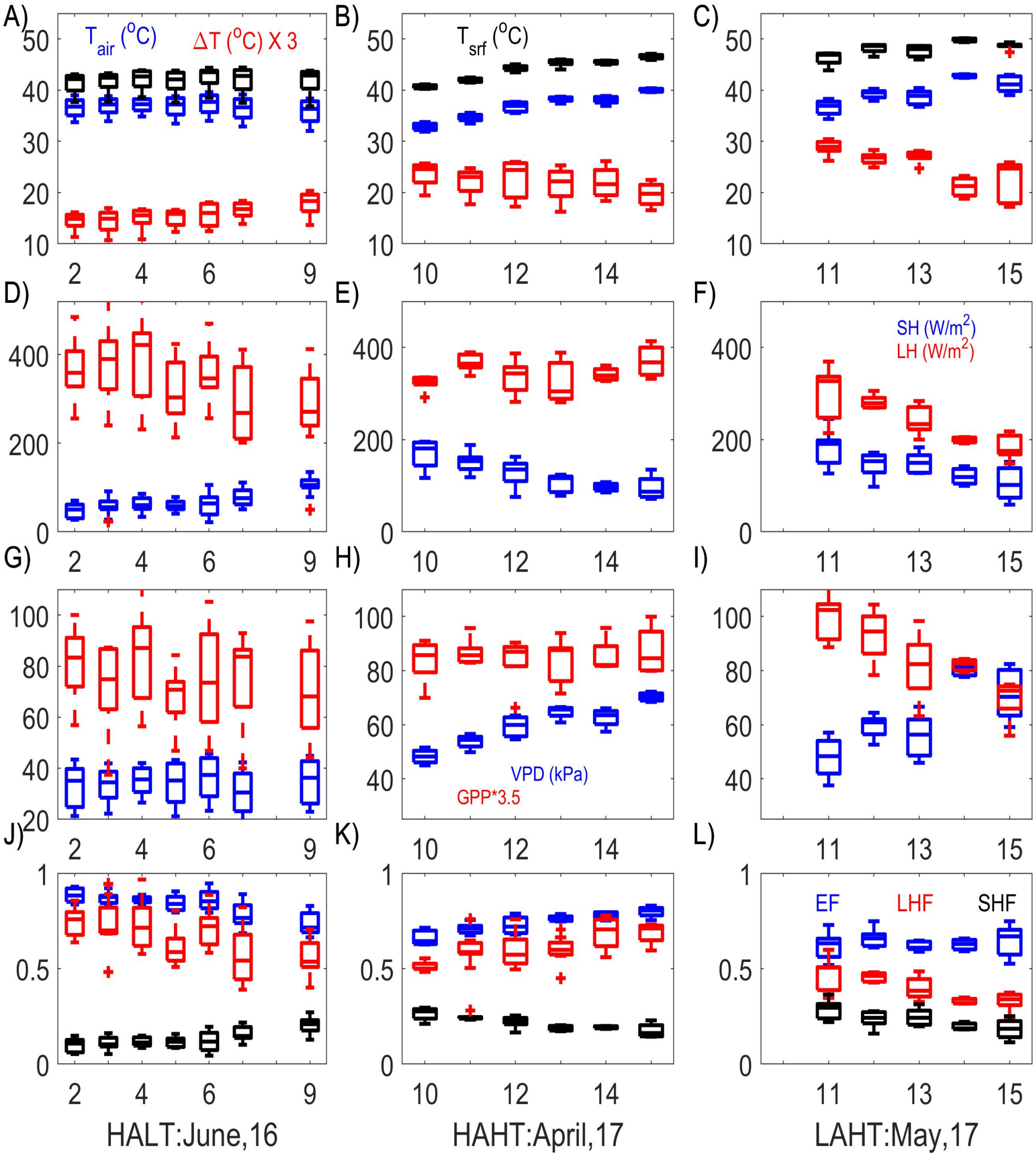


*Figure 3: Box plots showing the variations in near surface meteorology and surface fluxes during the cases. Row 1 illustrates Time series of midday (1100-1400 LT) variation in $T_{srf}$, $T_{air}$ and (-)ΔT values during HALT, HAHT and LAHT, respectively. Row 2 is same as Row 1 but for SH and LH. Row 3 is same but for VPD and GPP ; Row 4 is same but for EF, LHF (red) and SHF.*

https://doi.org/10.5194/acp-2021-40
Preprint. Discussion started: 1 June 2021

Atmospheric Chemistry and Physics Discussions

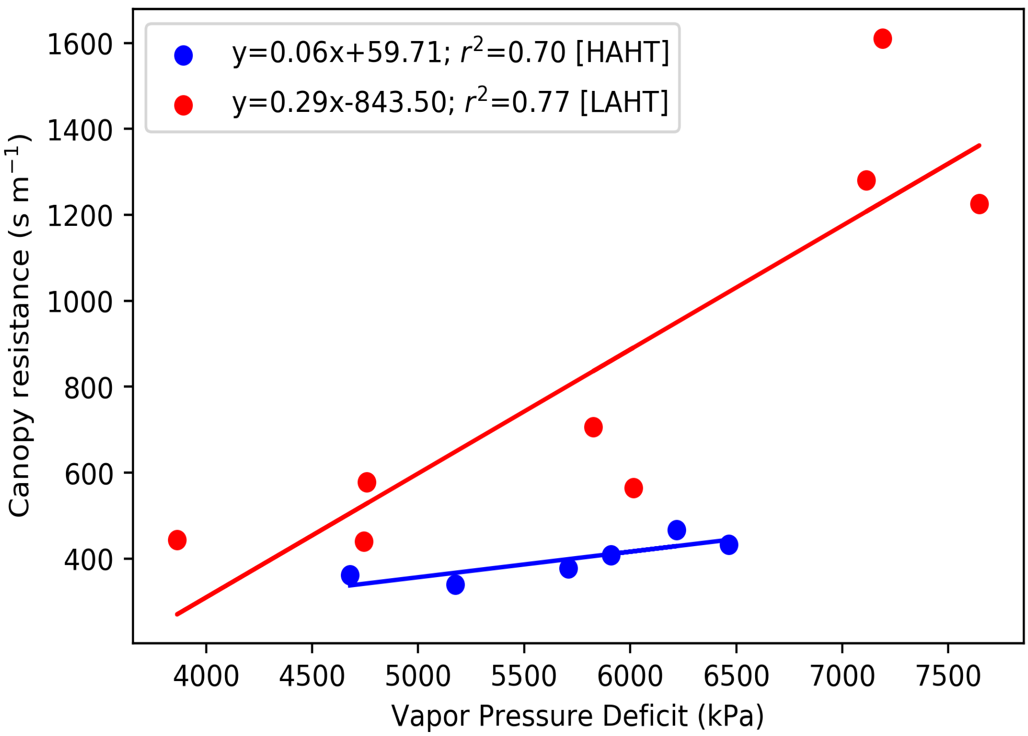


*Figure 4: Linear correlation between daily midday average Canopy resistance derived from Penman-Monteith equation and observed Vapor Pressure Deficit (VPD) for HAHT and LAHT cases*